# Analysis of the chemical composition and deposition mechanism of SiOX-ClY layer on the plasma chamber walls during silicon gate etching

Martin Kogelschatz, Gilles Cunge, Nader Sadeghi

# Analysis of the chemical composition and deposition mechanism of the $SiO_x-Cl_y$ layer on the plasma chamber walls during silicon gate etching

Martin Kogelschatz
*Laboratoire de Spectrométrie Physique, Université Joseph Fourier-Grenoble, BP 87, 38402 St. Martin d'Hères, France*

Gilles Cunge
*Laboratoire des Technologies de la Microélectronique, CNRS, 17 Rue des Martyrs (CEA-LETI), 38054 Grenoble Cedex 9, France*

Nader Sadeghi
*Laboratoire de Spectrometrie Physique, Université Joseph Fourier-Grenoble, BP 87, 38402 St. Martin d'Hères, France*

(Received 4 August 2003; accepted 23 February 2004; published 27 April 2004)

During silicon gate etching in low pressure high density $HBr/Cl_2/O_2$ plasma, $SiOCl_x$ layers are deposited on the reactor walls. These layers are at the origin of process drifts. However their chemical composition, deposition mechanism and their influence on the plasma chemistry remains poorly understood. In this study, the chemical composition of this layer has been investigated by a ''plasma etching-sputtering'' technique: the silicon oxychloride layer deposited on the reactor walls during the etching of a 200 mm diam silicon wafer has been subsequently submitted to an Ar plasma with the addition of a few % $SF_6$. During the slow etch process of this layer, time-resolved optical emission spectroscopy and mass spectrometry have been used to follow the time evolution of the gas phase concentration of different atoms and radicals, the etch products of the $SiOCl_x$ layer. The results give insight into the chemical nature of the deposited layer and of its variation as a function of the depth. In particular, it will be shown that these layers are chlorine-rich and not oxidelike. Also, their composition is not homogeneous through their depth. In a second set of experiments, the $SiOCl_x$ layer has been exposed to an $Ar/O_2$ plasma providing information on the oxidation mechanism of the Si–Cl bonds and thus on the $SiOCl_x$ film deposition mechanism in $HBr/Cl_2/O_2$ plasmas. This oxidation mechanism is acting through the entire volume of the 10 nm thick layers and proceeds by substitution of Cl atoms of SiCl bonds by O atoms, resulting in desorption of a large amount of Cl atoms from the chamber walls during the layer oxidation. Finally, the layer on the chamber walls has been exposed to an $Ar/Cl_2$ plasma, demonstrating that $SiOCl_x$ layers are not etched significantly by Cl atoms.  [DOI: 10.1116/1.1710496]

## I. INTRODUCTION

The influence of the plasma chamber walls on the plasma gas phase chemistry in high density discharges used for plasma processing remains one of the least understood aspects of the plasma–surface interaction. For different atoms and radicals produced in high density plasmas operating at low pressure, the rate of chemical reactions in the gas phase is usually much smaller than the rate of their diffusion to the chamber walls. Therefore, chemical processes occurring at the reactor walls, in conjunction with electron impact dissociation reactions in the gas phase, control the overall gas composition and plasma chemistry. In most discharges used for etching applications, the etch anisotropy results from deposition of a polymerlike layer on the trench side-walls. But a similar layer is also deposited on the reactor walls. The depositing process involves consumption of some plasma produced species (whose gas phase concentrations is thus damped) but can also result in the production of some other species at rates which may greatly exceed their formation rates by electron impact dissociation in the gas phase.[1] The chamber walls can therefore act either as sink or production region of reactive radicals, and changes in the chemical nature of the chamber walls' coating alter the rates of surface assisted reactions and lead to a process drift.

The process control and wafer to wafer process reproducibility is a very large issue in silicon gate etching (and shallow trench isolation formation). The tolerance in terms of critical dimension (CD) control shrinks with the gate dimension, being typically about 10% of the length targeted: the final dimension of a targeted 50 nm gate must be controlled within 5 nm. This nanometer-scale linewidth control can only be achieved by ensuring that the plasma properties such as electron temperatures, electron density and plasma composition are reproducible from wafer to wafer. In practice this is achieved either by conditioning the reactor walls (i.e., deposit always the same film) or by cleaning the film deposited on the walls from the previous process with an appropriate plasma chemistry before processing each wafer. To be efficient both of these approaches require a detailed understanding of the plasma–reactor walls interaction in the used chemistry.

Silicon gate etching is usually performed in low pressure high density $HBr/Cl_2/O_2$ plasmas. Thanks to the deposition of $SiO_x$-like passivation layers on the feature sidewalls, this chemistry provides highly anisotropic etching of silicon gates.[2–4] The exact mechanism is now well accepted to be the redeposition on the sidewalls of $SiCl_x$ etch products followed by their oxidation on the surface.[5] Since the deposition rate of the passivation layer on the gate and mask sidewalls directly drives the etched profile (by inducing a slope in the gate sidewalls), it is expected that any drift in the gas phase of $SiCl_xBr_y$, O and Cl species concentrations will result in different etched profiles and etch rates. For *a given process*, such changes may occur when the chemical composition of the coatings present on the chamber walls are modified by the plasma process being used.

During the gate etch process, the plasma is also depositing an oxychloride layer on the chamber walls.[6] Therefore, after processing a few wafers in a nominally clean reactor ($Al_2O_3$ walls) the chemical composition of the surfaces in contact with plasma changes progressively from $Al_2O_3$ to $SiO_xCl_y$. This is accompanied by a drastic decrease of the recombination probability of halogen atoms on the walls (and thus the dissociation degree of the plasma), with large consequences on the etched gate profile. For example, Xu *et al.*[7] reported that the Cl and Br atoms concentration can drop by more than 60% when changing from "clean" $Al_2O_3$ chamber walls to a passivated chamber with silicon oxide deposition on the alumina walls. Similar conclusions were also drawn by Chou *et al.*[8] and Ullal *et al.*[9] Therefore, it is well accepted that the halogen atoms recombination at the reactor walls can seriously alter the gas phase chemistry. Furthermore the atomic O concentration in the gas phase is also controlled by recombination[10] and abstraction reactions together with oxidation reactions of the layer on the wall and/or etching reaction of carbon-containing resist masks. As a result, changes in the chemical nature of the surface exposed to the plasma may change the O atoms concentration in the gas phase, which in turn may have a large impact on the $SiCl_x$ etch product gas phase concentration by modifying their surface loss probability. This effect has been predicted by Lee *et al.*[11] and observed experimentally by mass spectrometry experiments,[12] which have shown that the gas phase $SiCl_x$ species concentration decreases with increasing $O_2$ gas flow in a $HBr/Cl_2/O_2$ chemistry. This is because the oxidation rate of $SiCl_x$ deposited on the reactor walls increases (and thus their global sticking probility).

Therefore, chemical reactions taking place at the reactor walls can modify the plasma gas phase chemistry during a silicon gate etch process at low pressure. Since the species concerned ($SiCl_x$, O, Cl) are also those that control the etching profile and the etch rate, it is important to analyze the mechanisms responsible for the deposition and etching of $SiO_xCl_y$ layers on the chamber walls during the silicon etch process. This will allow to anticipate the influence of the external parameters on the plasma chemistry, and to develop appropriate cleaning and conditioning procedures for industrial reactors. This will also allow the improvement of the available plasma/feature profile evolution simulation tool.[13,14] Furthermore, information drawn from studies on the reactor walls are helpful in controlling the passivation layer thickness (thus the gate CD) which is governed by similar deposition mechanisms.

However, in contrast to passivation layers, the deposition and etching mechanisms of the $SiO_x$ layer on the vacuum vessel have been studied only very recently, and both the chemical nature of this layer, and its deposition mechanisms, and the influence of the layer on the plasma chemistry remain poorly understood. This is mostly due to a lack of *in situ* diagnostics for probing surface reactions at the walls. Recently, Godfrey *et al.*[15] have developed a specific diagnostic technique, the multiple total internal reflection-Fourier transform infrared spectroscopy (MTIR-FTIR) to study the chemical nature and deposition rate of the $SiO_xCl_y$ layer on the walls of an industrial reactor as a function of the rf bias power and $O_2$ gas flow in $Cl_2/O_2$ plasmas used for Shallow Trench Isolation (STI) applications. As a result, they demonstrated that the deposition mechanism is the oxidation of the redeposited $SiCl_x$ species and proposed a kinetic model for the film deposition rate.[6] They also demonstrated that oxychloride films can be eliminated with a $SF_6$ plasma[16] and discussed in detail the ion-enhanced etching mechanism of such layer in fluorine chemistry.

In the present article, we have studied the chemical composition of the layer deposited on the chamber walls during gate etch processes. For this purpose, the layer deposited during the $HBr/Cl_2/O_2$ plasma was subsequently etched by an $Ar/SF_6$ plasma. Time resolved optical emission spectroscopy (OES) and mass spectroscopy (MS) are then used to monitor the relative densities of the species desorbing from the walls, providing information on the layer composition as a function of its depth. Complementary information on the layer deposition mechanism are obtained by exposing the layer to an $Ar/O_2$ plasma, and the influence of Cl atoms on such layers was studied by exposing them to an $Ar/Cl_2$ plasma.

## II. EXPERIMENTAL SET-UP

Experiments were carried out in an industrial ICP source (LAM 9400). In all the experiments described below, the wafer temperature is kept at 65 °C by helium backside cooling (ESC chuck), while the anodised aluminum walls of the chamber are kept at 50 °C. The plasma is excited by feeding the antenna (lying on the quartz roof) with 13.56 MHz rf power, while the energy of the ions bombarding the wafer is independently controlled by a second 13.56 MHz rf power supply. Unless otherwise stated, in all the experiments described below, the plasma used to coat the chamber walls with a $SiO_xCl_y$ layer was a typical sub-100 nm gate etch process. It consists of a 5 mTorr total pressure, HBr (120 sccm)/$Cl_2$ (60 sccm)/$O_2$ (5 sccm) gas mixture excited with 300 W rf power and 90 W rf bias power (Table I). After 40 s of a 200 mm diam blanket silicon wafer etching step, reactive gases are pumped out, the silicon wafer is removed from the chamber and the reactor is filled with an

TABLE I. Plasma operating conditions.

| Plasma conditions | HBr (sccm) | $Cl_2$ (sccm) | $O_2$ (sccm) | Ar (sccm) | $SF_6$ (sccm) | Pressure (mTorr) | Source rf power (W) | Substrate | Bias rf power (W) |
|---|---|---|---|---|---|---|---|---|---|
| (1) $SF_6$ (120 s) | 0 | 0 | 0 | 0 | 50 | 5 | 600 | ··· | 0 |
| (2) $HBr/Cl_2/O_2$ (40 s) | 120 | 60 | 5 | 0 | 0 | 5 | 300 | Si | 90 |
| (3) $Ar/SF_6$ | 0 | 0 | 0 | 50 | 5 | 15 | 400 | ··· | 0 |
| (4) $Ar/Cl_2$ | 0 | 5 | 0 | 50 | 0 | 15 | 400 | ··· | 0 |
| (5) $Ar/O_2$ | 0 | 0 | 2 | 50 | 0 | 15 | 400 | ··· | 0 |
| (6) Ar | 0 | 0 | 0 | 50 | 0 | 15 | 400 | ··· | 0 |

$Ar/SF_6$ mixture at 15 mTorr (Table I) and excited with 400 W source rf power, no rf bias power. This $Ar/SF_6$ plasma chemically sputters the $SiOCl_x$ layer deposited by the previous process on the reactor walls and the time evolution of the etch products desorbing from the layer is followed by time-resolved plasma diagnostics. The plasma chamber is then cleaned in a pure $SF_6$ plasma for 2 min prior to the next experiment, allowing highly reproducible results to be obtained. In complementary experiments, small amounts of $O_2$ (2 sccm) or $Cl_2$ (5 sccm) are added to the Ar (50 sccm) plasma instead of $SF_6$. In all these experiments, the throttle between the plasma chamber and the turbomolecular pump was kept fixed to obtain 15 mTorr prior to the plasma strike. The pressure increased up to 25 mTorr at the beginning of the $Ar/SF_6$ discharge due to the dissociation of molecular species, gas heating and species production from the reactor walls, but decreased with decreasing etch product desorption. The plasma operating conditions are summarized in Table I.

During the silicon oxychloride layer etching in $Ar/SF_6$ plasma, the time evolution of the species concentration in the gas phase has been followed by both OES and MS. The system used for the OES consists of an UV grade optical fiber which injects the light collected from the plasma into a 60 cm focal length monochromator (Jobin Yvon HRS60) equipped with a 1200 grooves/mm grating blazed at 250 nm. The dispersed light is then detected by an amplified diode array (IOMA) that at each exposure covers about 30 nm, in the range of 200–900 nm. The spectral resolution of the system is better than 0.1 nm. The mass spectrometry system was a Hiden EQP working in the gas analyzing mode.[17] The gas was sampled through a 100 $\mu$m orifice located on the chambers' side wall and then ionized by 70 eV electrons for the mass analysis by the quadrupole.

In order to detect the temporal evolution of the intensity of the following transitions: Cl (725.4 nm), Br (679.0 nm), H (656.2 nm), O (777.4 nm), Si (302.0 nm), SiCl (280.9 nm),[18] and $Cl_2$ (258 nm),[19] emission spectra were taken every 0.5 s, during 120 s. So, at each wavelength position of the monochromator, we record 240 spectra, corresponding to different times. Consequently, the same experiment had to be repeated several times in order to acquire spectra for different spectral regions. In each case, the signal intensity was deduced from the integrated surface of the line (or band). These signals have then been normalized to the 675.4 nm argon line intensity. All integrated surfaces have been normalized by the acquisition time. All the emission signals presented in this work are given in arbitrary units but are scaled between different figures. Figures 1(a) and 1(b) show typical partial spectra of the 675 and 300 nm regions at different times after the plasma ignition.

Actinometry is expected to be reliable in this particular experiment since argon is the main gas. We did not use the Ar 750 nm line, which is recommended for the actinometry, because it was too intense compared to the intensity of other species lines. Comparing the time variation of the intensity of several infrared lines, including the 810 and 811.5 nm

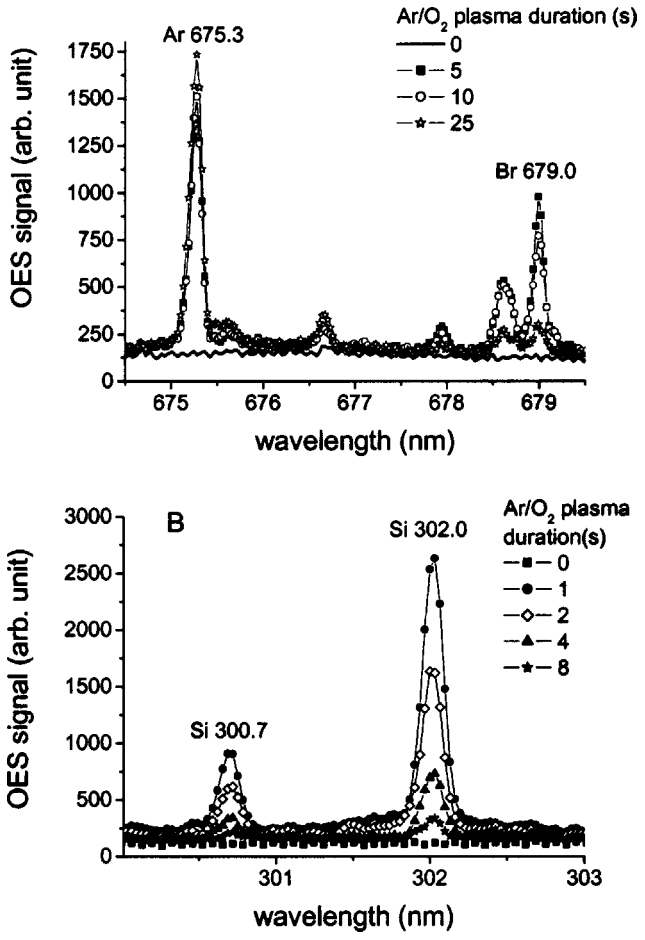


FIG. 1. Time dependent OES spectrum of the 675 (A) and 300 nm (B) regions in $Ar/O_2$ plasma.

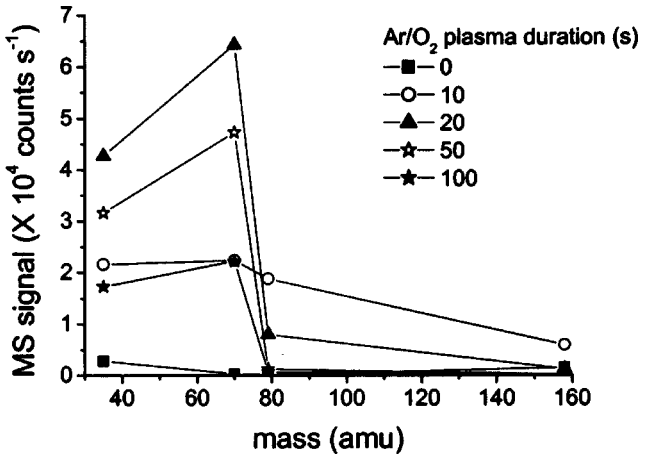


FIG. 2. Time dependent mass spectrum in $Ar/O_2$ plasma: Cl (35), $Cl_2$(70), Br (79), and $Br_2$(158).

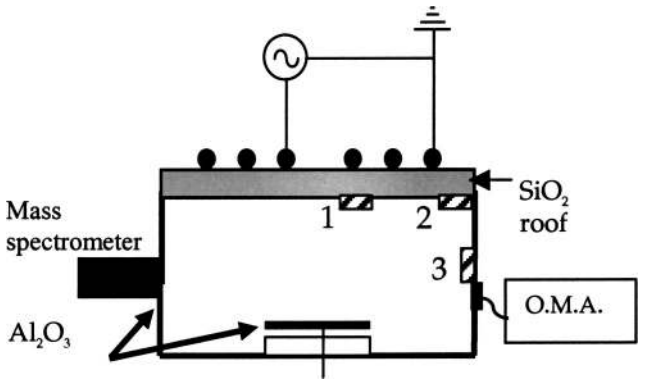


FIG. 3. Schematic of the plasma chamber and diagnostics. Numbers 1, 2, and 3 identify the locations where the net deposition rate of the $SiO_xCl_y$ layer has been measured and reported in Table II.

lines, we concluded that metastable atoms do not participate significantly to the excitation process. In fact, the upper level of the 811.5 nm line is known to be very efficiently excited from the metastable $Ar^*(^3P_2)$ state.[20] However, for Si, H, Cl, and O atoms, the signal intensity may in some cases originate from the dissociative excitation of molecules (i.e., HCl, $Cl_2$,…). We did not have the possibility to monitor the time evolution of the electron energy distribution function, so we assumed that it was negligible, even in the case of the $Ar/SF_6$ plasma, where the enhancement of the pressure was the most significant. To confirm the above assumptions, the actinometric signals of O and Cl were systematically compared to their mass spectrometric measurements, acquired simultaneously. In most cases, the results obtained by actinometry were in good agreement (but with a higher signal to noise ratio) with those deduced from mass spectrometry. Furthermore, anytime that was possible, the time evolution of several lines of the same species were recorded and then compared between them. The agreement was also good. Therefore, the relative variations of the atomic species concentrations were deduced from actinometry data.

In order to avoid complicated analysis of the MS data, polluted by cracking patterns of the heavier molecules,[21] the MS was mainly used to detect stable molecular species of the plasma (i.e., species whose ions are mostly produced from their parent molecules and not from the dissociation, inside the ionization chamber of the mass spectrometer, of heavier molecules. These molecules are: $Cl_2$, HCl, HBr, $Br_2$, BrCl, $SiCl_4$, $SiF_4$, and $O_2$. For chlorine and bromine containing species systematic analysis of the species isotopes has been carried out in order to correctly assign the observed masses to the corresponding species. Furthermore, in order to provide a good temporal resolution ($<1$ s), only five different masses were recorded at the same time. The masses were acquired in increasing order. So the same experiment had to be repeated several times in order to acquire the signal of all the species studied. Figure 2 shows a typical MS data. The points are connected with lines to guide the eye.

Finally, the deposition rate of the silicon oxychloride layer during the etching of a silicon wafer in the $HBr/Cl_2/O_2$ plasma and the etch rate of this layer in $Ar/SF_6$ plasma have been measured at several locations in the chamber. For these measurements, a 15 nm thick $Al_2O_3$ layer was deposited by Atomic Layer Deposition[22] on a 200 mm diam silicon wafer. This wafer was then cut into monitoring samples of $2.5\times2.5$ $cm^2$, which were then fixed at several locations in the chamber using adhesive kapton (see Fig. 3). The sample No. 1 was fixed on the quartz roof directly below the hot point of the rf antenna where the capacitive coupling to the plasma is the strongest (resulting in the highest kinetic energy of ions bombarding the reactor walls). Sample No. 2 was fixed on the edge of the quartz roof, where the capacitive coupling of the antenna is weak. Finally, a third sample (No. 3) was fixed onto the $Al_2O_3$ coated reactors' wall, at mid height between the bottom and the roof of the chamber. These three samples were then exposed to our standard deposition plasma (40 s $HBr/Cl_2/O_2$ in the presence of a Si wafer) and then removed from the chamber for *ex situ* layer thickness determination by spectroscopic ellipsometry and High Resolution Scanning Electron Microscope (SEM) from Hitachi Ltd. (S5000).

## III. RESULTS AND DISCUSSION

### A. $SiOCl_x$ layer deposition rate and etching rate

Table II shows the measured thickness of the silicon oxychloride layer deposited on the monitoring samples fixed at different parts of the chamber after etching a blanket silicon wafer in the $HBr/Cl_2/O_2$ plasma for 40 s. The locations where these measurement were done are shown schematically in Fig. 3, and the thicknesses indicated in Table II are those measured by the high resolution SEM (having an ac-

TABLE II. Measured $SiOCl_x$ layer thickness at three positions in the reactor, after deposition in $HBr/Cl_2/O_2$ plasma for 40 s, and after deposition followed by partial etching in $Ar/SF_6$ plasma.

| Plasma/$SiO_x$ layer thickness (nm) | Position 1 | Position 2 | Position 3 |
|---|---|---|---|
| $HBr/Cl_2/O_2$ (40 s) | 6 | 11 | 13 |
| $HBr/Cl_2/O_2$ (40 s) + $Ar/SF_6$ (11 s) | 0 | 7 | 10.2 |

curacy of about 2 nm). These numbers are in very good agreement (better than 30%) with spectroscopic ellipsometric measurements on samples. Schaepkens *et al.*[23] studied the effect of parasitic capacitive coupling through the dielectric window of inductively coupled fluorocarbon plasmas. They have shown that the quartz window erosion was largely nonuniform with a faster erosion at the coil position where a high peak to peak voltage was present on the coil. The quartz window etch rate was found to scale with both the ion flux (larger near the center of the quartz roof) and ion energy (large below the hot point of the coil). In our experiments, the ion flux and ion energy are thus expected to decrease from position 1 to position 2 and again to position 3. Indeed Table II shows that 13 nm thick $SiO_xCl_y$ layers are deposited at midheight on the floating $Al_2O_3$ reactor walls (position 3), while the thickness is reduced to 11 nm on the edge of the quartz roof (position 2) and finally 6 nm below the antenna on the quartz roof (position 1). This is demonstrating that the net deposition rate of the $SiO_xCl_y$ layer in $HBr/Cl_2/O_2$ plasma results from competition between etching and deposition, etching limiting the net deposition rate below the antenna coil, where the ion energy is the largest.

Also shown in Table II is the thickness of the silicon oxychloride layer remained on the monitoring samples after their exposure for 11 s to the $Ar/SF_6$ plasma (process 3) studied hereafter. As expected, the etch rate of the silicon oxychloride layer is the highest below the antenna, where the flux of energetic ions impinging on the walls is the largest. From the data of Table II, and assuming that at each position the etch rate of the layer in the $Ar/SF_6$ plasma is not time dependent, we conclude that the deposited $SiO_xCl_y$ layer will be completely removed from the different parts of the reactor walls at different times. First, the layer present below the inductive antenna will be cleared in less than 11 s; the layer deposited on the other parts of the quartz roof and that present on the upper part of the $Al_2O_3$ chamber walls (near position 2) are expected to be totally etched in about 30 s; finally, the layers deposited on the $Al_2O_3$ chamber walls (position 3) will require more than 45 s to be cleared. Therefore, during the etching of the silicon oxychloride layer in the $Ar/SF_6$ plasma, the chemical composition of the reactor walls in contact with the plasma is expected to be continuously changing during the mild $Ar/SF_6$ etching process and the area of $Al_2O_3$ exposed to the plasma will increase with time.

These changes in the reactor walls chemical nature could be tracked by following changes in the relative $Cl_2$ to Cl concentration ratio in *a given* $Cl_2$ based plasma but with various initial wall conditions.[9] In fact, this ratio should evolve during the $Ar/SF_6$ plasma because the recombination coefficient $\gamma$ of Cl atoms is much larger on $Al_2O_3$ surfaces than on $SiO_2$-like surfaces.[24] In Fig. 4 we have plotted the ratio of the $Cl_2$ to Cl emission intensity measured on the 258 nm continuum and the 725 nm line both in a perfectly clean reactor ($Al_2O_3$ walls plus $SiO_2$ quartz roof), in a $SiO_xCl_y$ passivated reactor (after 40 s of $HBr/Cl_2/O_2$ plasma) and in a "partially clean" reactor that is to say after different etching times of the $SiO_xCl_y$ layer in an $Ar/SF_6$ plasma. For this particular experiment, we used an $Ar/Cl_2$ (20/50 sccm) plasma at 5 mTorr, 400 W source power and without bias power ($Al_2O_3$ ES-chuck without wafer). As expected, since the value of $\gamma$ for Cl atoms is much larger on $Al_2O_3$ than on $SiO_x$, the ratio of the $Cl_2$ to Cl emission is more than six times larger in a clean reactor than in a $SiO_xCl_y$ passivated chamber. This result corroborates other data reported in the literature[7,9] and illustrates well the issue of process drifts associated with changing reactor walls conditions. Furthermore, the influence of the $Ar/SF_6$ plasma duration on the Cl atoms recombination rate is in good agreement with the above discussion. For times shorter than 20 s, only the layer deposited on the quartz roof will be cleared, while most of the $Al_2O_3$ surfaces are kept covered by a silicon oxychloride: during that time, the plasma sees essentially an oxide like reactor, and the recombination rate of Cl atoms is roughly constant. By contrast, for times longer than 20 s, the $Al_2O_3$ reactor wall is partially cleaned (most probably the upper part of the walls, near point 2 in Fig. 3) and the $Cl_2$ to Cl ratio increases as the $Al_2O_3$ area exposed to the plasma increases. The etch rate of the layer on the walls is slow, and more than 90 s of the $Ar/SF_6$ plasma are required to clean the entire vessel and restore the $Cl_2$ to Cl emission ratio to its value obtained in a perfectly clean chamber.

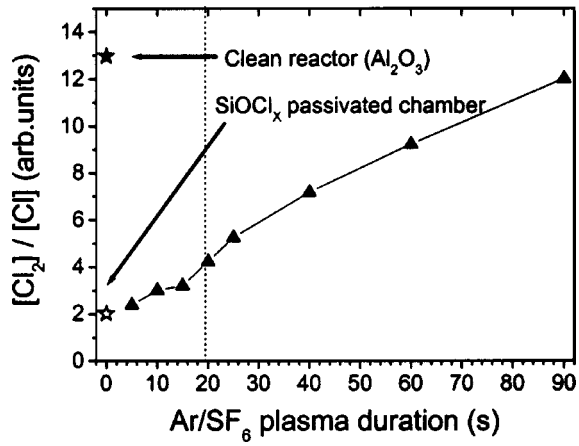


FIG. 4. Ratio of the $Cl_2$ to Cl concentration, deduced from the emission intensity of the 258 nm $Cl_2$ continuum and 725 nm Cl line, respectively, for various wall conditions. (★) in a clean reactor, (☆) in a $SiO_xCl_y$ totally passivated chamber, and (▲) in a partially coated chamber resulting from the removal of the layer with an $Ar/SF_6$ plasma run for different periods.

Based on these results, it is now possible to analyze the time-dependent behavior of the species desorbing from the reactor walls during the layer etching in $Ar/SF_6$.

### B. $SiO_xCl_y$ layer ion-enhanced chemical etching in $Ar-SF_6$

#### *1. Contribution of the different parts of the reactor walls to the observed signal*

In the first set of experiments, the silicon oxychloride layer deposited on the chamber walls by the 40 s long $HBr/Cl_2/O_2$ plasma has been etched by the Ar (50 sccm)/$SF_6$(5 sccm) plasma. Figures 5, 6, and 7 summarize the tem-

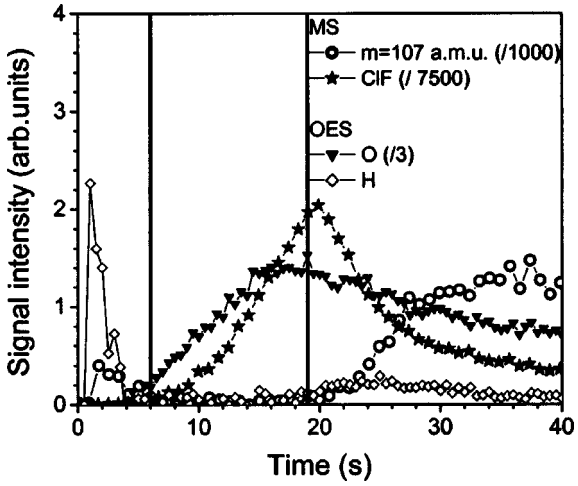


FIG. 5. Time dependent behavior of O, H, ClF and $m=107$ amu (probably $Al_2O_2FH_2$) during the layer etching in the $Ar/SF_6$ plasma (process 3). The vertical lines indicate approximately the endpoints for the film clearing below the antenna and on the entire quartz roof (6 and 19 s, respectively).

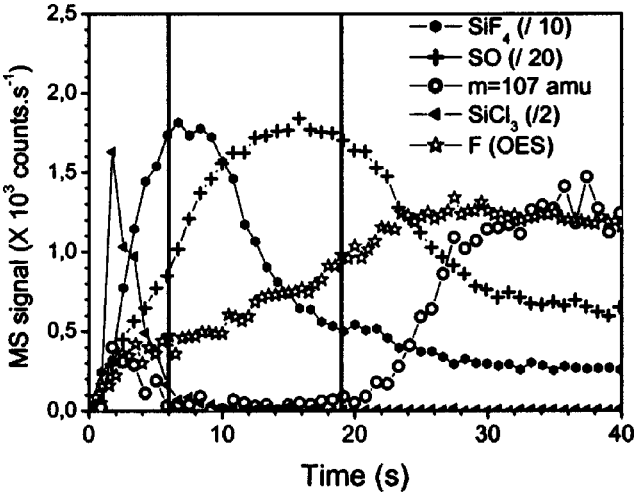


FIG. 7. Same as Fig. 5 but for silicon and oxygen containing species.

poral evolution of the concentration of different species detected in the gas phase during this etching step underlying the complexity of the silicon oxychloride film etching reactions. We should point out that in MS detection of neutrals, there is some ambiguity in attribution of ions selected by the MS and the neutral molecule from which they originate. Identification of molecules R reported in Figs. 5–7 correspond to the detection of $R^+$ ions. If for some radicals this assignment can be doubtful, for diatomic molecules and for $SiF_4$ there is a high probability that the ion comes from the corresponding molecule.

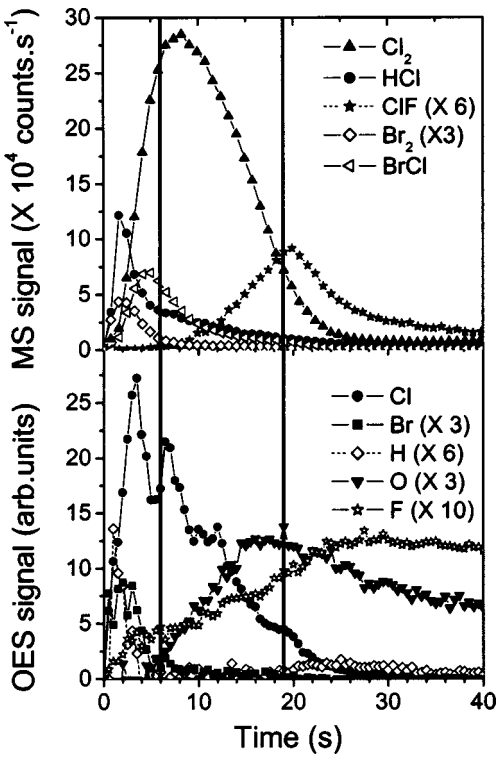


FIG. 6. Same as Fig. 5 but for halogen containing species.

As expected from the above discussion, several "end points" can be seen in Fig. 5, corresponding to the silicon oxychloride film elimination from different locations in the chamber. These end point times are pointed by vertical lines on this figure. To begin with, after 5–6 s of etching in the $Ar/SF_6$ plasma, O atoms and ClF molecules start to be detected in significant concentrations in the gas phase. As discussed above, this time is reasonably correlated to the time at which the layer starts to be cleared from the quartz roof below the powered region of the antenna. At this position, the incident ion energy is high and as soon as the $SiO_xCl_y$ layer is cleared, the chemical sputtering of the quartz roof will produce O atoms,[25] introduced into the gas phase. The fast removal of the $SiO_xCl_y$ layer below the antenna may also participate to the production of O atoms. However, O atoms are not detected during the first 4 s of etching. This could be an indication that the *surface* of the $SiO_xCl_y$ layer deposited below the antenna is O deficient and not oxide like. This point will be discussed in the next sections.

Secondly, another "end point" is indicated in Fig. 5 at 18–20 s. At this time, H emission increases together with the signal intensity at mass 107 amu (possible attribution to $Si_2O_2F^+$ or $Al_2O_2FH_2^+$ ions) in the mass spectrometer. Isotopic deconvolution shows that mass 107 amu can be separated in two contributions: SiBr etch products for times shorter than 10 s, and another species for times longer than 18 s. After a slow increase the signal at mass 107 amu stabilizes after 30 s which corresponds to the time required to remove completely the $SiO_xCl_y$ layer from the entire quartz roof area. However, the species at mass 107 amu cannot be unambiguously assigned to an etch product of the quartz roof otherwise it would rise as soon as the quartz roof starts to be exposed to the plasma (6 s) and not after 20 s.

Therefore it is reasonable to assume that the mass 107 is an etch product of the alumina walls and that the rapid rise of the signal at mass 107 amu at time 20 s corresponds to the

apparition of $Al_2O_3$ surfaces in contact with the plasma. From this observation the 107 amu signal could possibly be assigned to the $Al_2O_2FH_2$ molecule. This surface is most probably the upper part of the reactor walls where the layer etch rate is similar to that measured on the edge of the quartz roof (see Fig. 3 and Table II). This hypothesis is coherent with the observed slope enhancement of the $Cl_2$ to Cl concentration ratio after about 18 s in Fig. 4. After that time the behavior of the H atom signal intensity in Fig. 5 is an indication that H atoms are present at the interface between the $Al_2O_3$ wall and the $SiO_xCl_y$ layer. They can originate from water vapor, or can be chemisorbed at the surface of the alumina walls during the first few seconds of the $HBr/Cl_2/O_2$ silicon etching plasma.

As a summary, etch products introduced into the $Ar/SF_6$ plasma originate from several regions of the chamber: the layer deposited on the middle of the $Al_2O_3$ sidewall of the reactor (position 3 in Fig. 3) is etched at all times between 0 and 50 s; those parts of the quartz roof which are not lying directly under the antenna, together with the upper part of the $Al_2O_3$ reactor walls (position 2 in Fig. 3) are only contributing from time 0 to 30 s; finally, the $SiO_xCl_y$ layer from the portion of the quartz roof set just below the rf coil will produce species only during the first 8 s of the process. After that time, this latter portion will continue to produce species from the slow erosion of the quartz roof itself (most probably $SiF_4$ and $O_2$).

### 2. Other species detected during the $SiOCl_x$ film etching in $Ar/SF_6$ and Cl content in the layer

The etching mechanisms of the silicon oxychloride film by $SF_6$ plasmas have been discussed in detail by Ullal *et al.*[16] They have shown that after the $SF_6$ plasma was ignited, F atoms were first incorporated in the bulk of the film where they replace Cl atoms, and that the etching of the film proceeds only after this incorporation step. They suggest a two step mechanism for the film fluorination in which a F atom first abstracts a Cl atom from the Si–Cl bond (forming ClF in the gas phase) followed by a subsequent passivation of the Si dangling bond by a second F atom:

$$O_3Si{-}Cl_{(s)} + 2F_{(g)} \rightarrow O_3Si{-}F_{(s)} + ClF_{(g)}. \quad (1)$$

Figures 6(a) and 6(b) show the time evolution of the concentrations of halogen atoms and molecules during the layer etching in the $Ar/SF_6$ plasma. We observe that F atoms, resulting from the dissociation of $SF_6$, are consumed by the film for the first three seconds after the plasma ignition. This is evidenced by the low F atoms concentration and little $SiF_4$ production, (as seen in Fig. 7) for $t<3$ s. However, we do not observe any production of ClF molecules during this period. Instead, Fig. 6(a) shows that recombination and abstraction reactions of atomic species during the fluorination of the layer and its etching are producing successively HCl, BrCl, $Cl_2$ and finally ClF molecules. The rapid build-up of the atomic Cl concentration during the initial film fluorination [Fig. 6(b)] suggests that F incorporation into the film proceeds by direct substitution to Cl atoms in Si–Cl bonds and not through an abstraction mechanism,

$$(SiO_xCl_y)_{bulk} + (F)_g \rightarrow (SiO_xCl_{y-1}F)_{bulk} + (Cl)_g. \quad (2)$$

In this scheme, F atoms can diffuse deeply (several monolayers) into the silicon oxychloride film and produce chlorine atoms in the volume, which can then diffuse through the silicon oxychloride layer and reach the surface. These chlorine atoms can then either recombine at the layers' surface prior to be desorbed, or alternatively desorb directly in the plasma gas phase where they diffuse prior to undergo recombination or abstraction reactions with Cl, H, Br or F atoms at another location on the reactor walls. Since the SiH bond energy [$<3.06$ eV (Ref. 26)] is much lower than that of SiCl and SiBr ($4.03\pm0.6$ eV and $3.68\pm0.7$ eV,[27] respectively), it is likely that Cl atoms will first abstract H atoms from the surface and not the contrary. A similar conclusion was drawn by Greer, Coburn, and Graves[28] for the F abstraction of H atoms on the photoresist. In any case, the kinetic of formation of HCl is faster than that of $Cl_2$: the $SiO_xCl_y$ film surface is rich in H atoms left from the $HBr/Cl_2/O_2$ plasma, and once this H-rich layer has been etched and H atoms eliminated from the reactor volume by gas pumping, the HCl production stops in favor of BrCl and $Cl_2$ production. Similarly, all the Br-containing molecules are detected only at the beginning of the $Ar/SF_6$ etching plasma, suggesting that Br atoms are mostly present in the first monolayers of the surface. As a result, BrCl molecules are formed mostly during the first 10 s of the $Ar/SF_6$ plasma.

The fact that ClF only appears in the gas phase when the quartz of the roof comes into contact with the plasma is puzzling. Since the reactor wall surface is largely chlorinated, and since both F and Cl atoms are present in the plasma gas phase from the beginning time zero, ClF formation through the abstraction reactions of Cl atoms of the surface could occur immediately in the plasma strike. Therefore, either ClF abstraction reactions have a much larger rate on $SiO_2$ surfaces than on $SiO_xCl_y$ surfaces or, alternatively, F atoms, originating from the chamber cleaning in pure $SF_6$ (process 1; Table I) prior to each run, are embedded in the quartz roof below the layer. These F atoms can be abstracted by Cl atoms when the quartz roof starts to be exposed to the plasma. After that time, in both cases the ClF concentration will increase proportionally to the quartz roof area exposed to the plasma until the ClF production becomes limited by the Cl atoms concentration in the gas phase ($t>20$ s).

Therefore, during the fluorination of the layer, a significant amount of Cl atoms is desorbed from the walls, demonstrating that the oxidation of silicon oxychloride etch products on the chamber walls during the $HBr/Cl_2/O_2$ plasma is largely incomplete, and that many Si–Cl bonds are embedded in the film. In order to estimate the chlorine content of the film deposited by the $HBr/Cl_2/O_2$ plasma, the mass spectrometer has been calibrated to convert the $Cl_2$ signal intensity into equivalent $Cl_2$ gas flow desorbing from the walls. This has been done *without plasma*, by measuring the ampli-

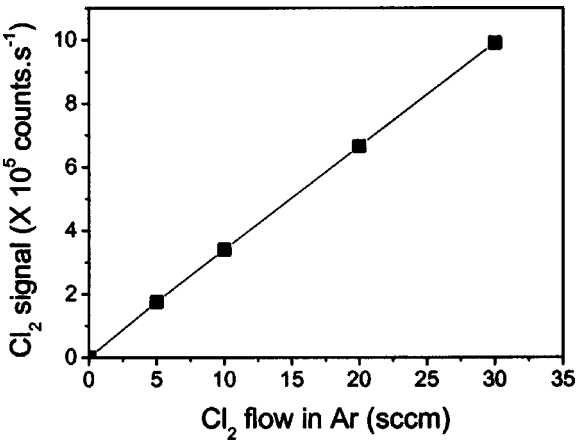


FIG. 8. Variation of the MS $Cl_2$ signal (70 amu) as a function of $Cl_2$ gas flow in Ar (50 sccm) at 15 mTorr.

tude of the 70 amu signal with the MS for different flows of $Cl_2$ gas added to 50 sccm Ar gas at 15 mTorr and constant pumping speed.

The result is shown in Fig. 8 from which we deduce that the amount of $Cl_2$ observed at the maximum of the signal in Fig. 6(a) ($t \approx 8$ s) is equivalent to 8.5 sccm of $Cl_2$ gas flowing into the chamber. The time dependent signal of $Cl_2$ in Fig. 6(a) can then be converted from count.$s^{-1}$ to molecule.$s^{-1}$ ($1\ \text{sccm} \equiv 4.48 \times 10^{17}$ molec.$s^{-1}$), and finally be integrated over the time and multiplied by 2 to yield the total number of Cl atoms generated in the gas phase during the etching of the oxychloride layer. From this calculation we deduced that at least $1 \times 10^{20}$ chlorine atoms were present in the film and detected as $Cl_2$ by mass spectrometry during the layer etching. This number is in fact a lower limit because Cl atoms present in the gas phase as a single radical or incorporated in another molecule than $Cl_2$ are not taken into account. As shown in Figs. 6(a) and 7 other chlorine containing species like HCl, ClF, BrCl, and $SiCl_x$ (only $SiCl_3$ shown) are also present in the gas phase of the $Ar/SF_6$ plasma. However, even with this lower limit number, and assuming that the film is uniformly deposited on the 4000 $cm^2$ of the chamber walls surfaces and its mean composition is $SiOCl_3$ with a density of 1.5 g.$cm^{-3}$ (similar to that of liquid $SiCl_4$), we calculate a film thickness of about 14 nm. This value coincides with the thickness of the layer deposited on the probe sample that was fixed on the side wall of the reactor (Sec. III A and Table II). Clearly, the film is not precisely $SiOCl_3$ but since the measured layer thickness deposited in the $HBr/Cl_2/O_2$ plasma is about 10–13 nm, this allows us to conclude that the deposited oxychloride film contains a very large amount of chlorine, which is a consequence of the low $O_2$ gas flow rate used during the deposition step. This is in good agreement with XPS analysis of the passivation layer deposited on the gate sidewalls under similar conditions,[29] which are indicating that the concentration of Cl in the passivation layer is typically 50%. Finally, we underline that the total number of Cl atoms detected as $Cl_2$ in Fig. 6(a) represents approximately 5% of the total number of $Cl_2$ molecules introduced into the reactor (60 sccm) during the 40 s of the $HBr/Cl_2/O_2$ silicon etching process.

Figure 7 shows the time evolution of the gas phase concentration of several etch products during the silicon oxychloride layer etching in the $Ar/SF_6$ plasma. First of all it shows that during the layer fluorination, the ion bombardment of the layer is producing $SiCl_4$ molecules detected as $SiCl_3$ in the mass spectrometer head.[21] These species probably originate from the layer below the antenna (position 1 in Fig. 3) where the ion energy is large (desorption of $SiCl_x$ requires ion bombardment while $SiF_4$ can desorb spontaneously).[30] This production however drops rapidly in favor of $SiF_4$ molecules, which after a few seconds become the predominant etch product of the silicon oxychloride layer. The $SiF_4$ signal intensity rises rapidly and reaches a maximum at the first "endpoint" when the $SiO_2$ quartz roof is reached below the antenna. The etching of the quartz roof itself is producing only small amounts of $SiF_4$ as evidenced by the low value of the $SiF_4$ signal intensity for times longer than 40 s when the $SiO_xCl_y$ layer will be removed from the walls. This means that the etch rate of the $SiO_2$ quartz roof is much smaller than the etch rate the chlorine-rich $SiO_xCl_y$ layer deposited on this roof. Therefore the decrease in the $SiF_4$ concentration observed between 10 and 18 s in Fig. 7 can be attributed to a decrease of the $SiO_xCl_y$ layer area exposed to the plasma as the layer on the quartz roof is progressively cleared. During these first 20 s, the layer present on the side chamber walls produces also $SiF_4$, thus contributing to the observed signal intensity. However, this contribution should be small because the etch rate of the $SiO_xCl_y$ layer on the side wall is smaller than that near the source region. The amount of this contribution is roughly given by the $SiF_4$ signal at 25 s in Fig. 7, i.e., when the quartz roof is totally cleared. Finally, as seen in Fig. 7, while the film is cleared from the different parts of the chamber vessel, the concentration of F atoms in the gas phase increases because they are less loaded in etching reactions.

Figure 7 also shows the time evolution of the signal from SO molecules. This species is believed to be an etch product from the $SiO_xCl_y$ layer and the quartz window. Indeed a systematic search by mass spectrometry of the $SiO_2$ etch products (such as $SiO_xCl_y$ or $SiO_xF_y$) in our $Ar/SF_6$ plasma was unsuccessful. This leads us to conclude that only O, $O_2$, and $SO_x$ molecules, which indeed have a similar time dependent behavior, are produced in significant quantity during the film etching by this plasma. However, although O atoms are only detected for times longer than 6 s, SO molecules appear as soon as the plasma strikes, suggesting that SO is an important etch product of the silicon oxychloride layer. Therefore, the increase of the SO signal from the gas phase during the first 10 s of the plasma can be attributed to a gradient of oxygen concentration in the $SiOCl_x$ layer, its surface being rich in Cl, but also in H and Br, and O deficient, while it is more oxidized and less chlorinated deeper. Indeed, this hypothesis is also coherent with the time dependent behavior of the O atoms concentration in Fig. 6(b): it rises during 10 s, then passes through a maximum near the quartz endpoint (20 s) and then decreases again. Clearly, if O atoms were pro-

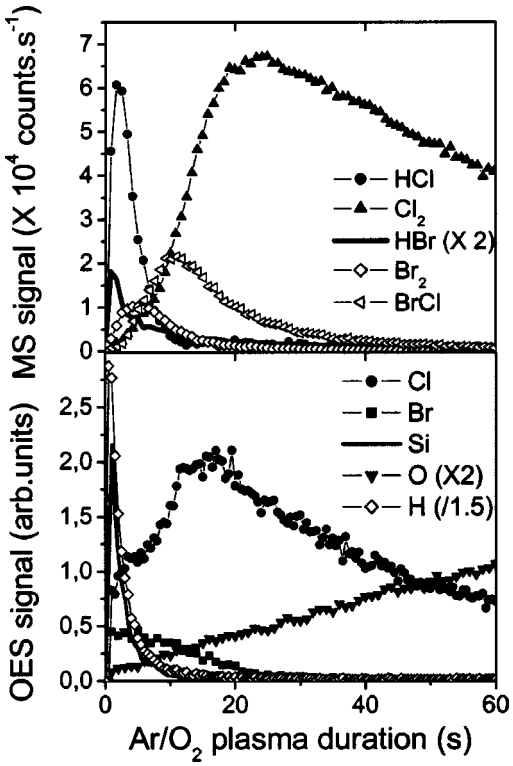


FIG. 9. Time dependent behavior of the gas phase concentration of several species during the $SiO_xCl_y$ layer exposition to an $Ar/O_2$ plasma (process 5).

duced only from the sputtering of the quartz roof, the signal should increase proportionally to the area of the quartz roof exposed to the plasma and thus reach a plateau value at about 20 s. However the observed signal is decreasing significantly after this end point demonstrating that a part of the signal comes from the sputtering of the $SiO_xCl_y$ layer on the chamber walls. Now, if the layer was homogeneous through its thickness, the contribution of the reactor walls to the observed O atoms signal intensity should be almost constant during the first 20 s, which is clearly not the case. Therefore we conclude that there is an increase in the amount of O atoms incorporated in the layer when going deeper from its surface. A possible explanation for this phenomenon will be discussed in the next paragraph.

At this point, we come to the conclusion that the deposited oxychloride layer is chlorine rich although these layers are often considered to be oxide like. In the next section we will thus discuss the oxidation kinetic of the silicon oxychloride layer by exposing this layer to a diluted $Ar/O_2$ plasma.

### C. $SiO_xCl_y$ layer oxidation in $Ar–O_2$ plasma

Figure 9 shows the time evolution of the concentration of several species detected in the gas phase during the first 60 s of the exposition of the silicon oxychloride layer to the $Ar/O_2$ plasma (see Table I for plasma conditions).

To begin with, since the Si and SiCl (not shown for clarity) signal intensities are small and drop rapidly to zero, we can conclude that the silicon oxychloride layer is not etched significantly under these conditions. This fast decay of the silicon containing etch products is attributed to the silicon oxychloride layer oxidation which changes the "reactive" $SiO_xCl_y$ surface layer into a more sputtering-resistant $SiO_2$ like layer. Indeed during the layer oxidation, the atomic O concentration is increasing monotonously demonstrating that at the beginning of the plasma most of the O atoms are pumped by oxidizing reactions in the $SiO_xCl_y$ layer. Figure 9 also shows that this is accompanied by a significant production of Cl and Br containing species. Again, we observe that HCl molecules are formed first, followed by BrCl and $Cl_2$. As previously discussed in the $Ar/SF_6$ case, this is also suggesting that the oxidation mechanism of etch products on the reactor walls proceeds by substitution of O atoms to Cl atoms of the Si–Cl bonds,

$$(SiO_xCl_y)_{bulk}+(O)_g \rightarrow (SiO_{x+1}Cl_{y-1})_{bulk}+(Cl)_g . \qquad (3)$$

According to this mechanism, Cl atoms are liberated from the silicon oxychloride layer due to oxidation. A similar behavior is observed for Br atoms, although the production starts to decay much sooner since Br atoms are mostly present at the surface of the layer as discussed previously. There are two possible explanations for this density gradient, either the production of BrCl molecules by abstraction reactions as discussed in the next section, or that the Si–Br bonds may be more efficiently oxidized than Si–Cl bonds thus eliminating Br atoms from the layer as it grows. Indeed, Desvoivres *et al.* have reported that the substitution of O to Br atoms in $SiOBr_x$ layer takes place when exposing the passivation layer to an oxygen-rich plasma.[31]

Although not shown in Fig. 9, the $Cl_2$ signal decreases down to zero after approximately 180 s. Once again, we can deduce the total amount of chlorine produced in the gas phase by integrating the $Cl_2$ signal over the 180 s exposition of the layer to the $Ar/O_2$ plasma. We find nearly the same amount of Cl atoms that was produced during the layer etching in the $Ar/SF_6$ plasma. Therefore, neglecting the contribution of HCl, BrCl, and other Cl containing species we can conclude that 3 min of $Ar/O_2$ plasma fully oxidizes (transforms to $SiO_x$) the initial silicon oxychloride layer. In particular, this means that O atoms can diffuse efficiently through the entire layer (about 10 nm thick in average) and oxidize the Si–Cl bonds deeply in the layer, liberating Cl atoms which can diffuse back to the gas phase. This mechanism is rather different than a surface oxidation mechanism and has several consequences on the deposition mechanism of silicon oxychloride layers in the $HBr/Cl_2/O_2$ plasma. In particular, since O atoms can diffuse through the layer, we expect that the "bottom" of the layer (in contact with the walls), that has been exposed for a longer time to O atoms of the depositing $HBr/Cl_2/O_2$ plasma, will be more oxidized than its surface. Therefore as discussed in the previous section, we expect concentration gradients of O and Cl atoms through the layer thickness, its surface being Cl-rich while it is more oxidized deeper. This conclusion is in good agreement with the observed evolution of O and SO signals discussed in Sec. III B.

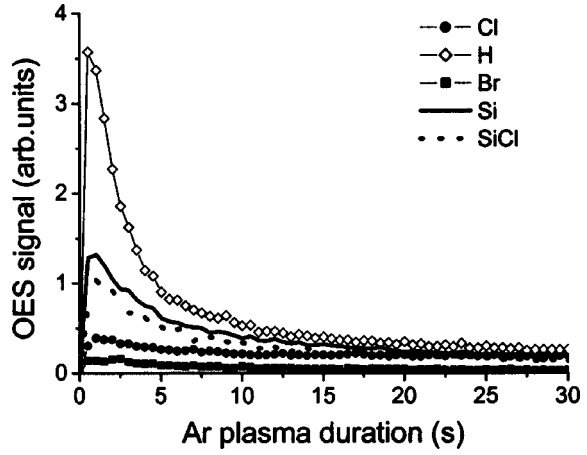


FIG. 10. Time dependent behavior of the gas phase concentration of several species during the $SiOCl_x$ layer exposition to a pure Ar plasma (process 6).

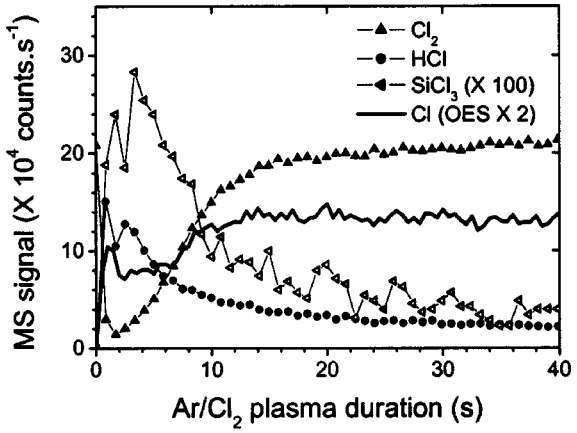


FIG. 11. Time dependent behavior of the gas phase concentration of several species during the $SiOCl_x$ layer exposition to an $Ar/Cl_2$ plasma (process 4).

The presence of this density gradient is also confirmed by results presented in Fig. 10, which shows the time variation of several species densities in the gas phase produced by physical sputtering of the $SiO_xCl_y$ layer in a *pure argon plasma*. In this case, the nonreactive $Ar^+$ ion bombardment only sputters species present near the surface of the layer. Signals of Si, SiCl, Cl, H, and Br reach their maximum values immediately on the plasma strike. This is interpreted by the larger amount of Si–Cl bonds on the top surface layer, easily sputtered by $Ar^+$ ions. The slow decay of these signals reveals the more sputtering resistant nature of the deeper layers which indicates a larger density of Si–O bonds. The decay of Si and SiCl signals is much faster in the $Ar/O_2$ plasma than in the Ar plasma due to a much lower sputtering rate of the layer resulting from its surface oxidation. The faster decay of the Br and H signals compared to the Cl signal confirms that these species are mainly present at the surface of the layer.

Regarding the influence of the reactor walls on the plasma chemistry in $HBr/Cl_2/O_2$ plasmas, such a deep oxidation mechanism has another important consequence: during a gate etch process the entire area of the reactor walls acts as an extra source of Cl atoms, produced by oxidation of the Si–Cl bonds of the whole $SiO_xCl_y$ layer deposited on the reactor walls. Therefore the larger the $O_2$ flow in the process the larger the Cl atoms production by the walls will be (until etch stop occurs). This may explain why at low $O_2$ gas flow the silicon etch rate increases with the amount of oxygen flow in $HBr/Cl_2/O_2$ plasmas.[32,33] Increasing the amount of O atoms in the plasma will enhance the surface production of Cl atoms from the deposited layer on the wall and thus their gas phase concentration. Indeed, we have recently reported that increasing the $O_2$ flow rate in $HBr/Cl_2/O_2$ chemistries is accompanied by a large increase of the Br and Cl concentrations in the gas phase.[12]

### D. $SiOCl_x$ layer exposition to $Ar–Cl_2$ plasma

Finally, in a last set of experiments the silicon oxychloride layer deposited on the reactor walls has been exposed to an $Ar/Cl_2$ plasma. In $HBr/Cl_2/O_2$ plasmas the $SiO_xCl_y$ layer net deposition rate on the chamber walls results from the competition between etching by Cl and Br atoms of redeposited $SiCl_x$ etch products and the oxidation of these etch products prior to their incorporation to the growing film. Thus, this experiment brings some information on the etch rate of this layer by Cl atoms. Figure 11 shows the time dependent behavior of HCl, $Cl_2$, and $SiCl_3$ species during the $SiO_xCl_y$ layer exposition to the $Ar/Cl_2$ plasma (see Table I for plasma conditions). The density of $Cl_2$ molecules, present in the gas mixture prior to the plasma ignition, decreases dramatically due to its electron impact dissociation. The resulting Cl atoms are then consumed on the reactor walls by abstraction and etching reactions, producing HCl, BrCl (not shown) and $SiCl_x$ etch products as shown in Fig. 11. However, both HCl and BrCl production drops rapidly because H and Br are present only near the surface of the layer. Furthermore, in Fig. 11 the $SiCl_x$ concentration also drops rapidly, indicating a significant decrease of the surface loss rate of Cl atoms during the first 10 s of the discharge. As a result of the larger number of Cl atoms available for recombination, the $Cl_2$ density increases with time.

In order to analyze more precisely the influence of the $Ar/Cl_2$ plasma on the $SiO_xCl_y$ layer, we have compared the time evolution of the species detected in the gas phase during the etching in $Ar/SF_6$ plasma of the as-deposited $SiOCl_x$ layer (identical to Figs. 6 and 7) and that of the same species under the same condition but after having exposed the layer for 1 min to an $Ar/Cl_2$ plasma. The comparison is shown in Fig. 12.

First, Fig. 12 shows that the layer etching end point on the quartz roof, as defined in Sec. III B (see mass 107 amu), is the same in both cases. Furthermore the amount of silicon desorbing from the layer in the form of $SiF_4$ is also almost similar in both cases showing that Cl atoms do not remove significantly the $SiO_xCl_y$ layer. More interesting, Fig. 12(a) shows that the as-deposited layer is producing $SiCl_x$ etch products (only $SiCl_3$ shown) during the first few seconds of the $Ar/SF_6$ plasma although only $SiF_4$ is detected when the layer has been preliminary exposed to the $Ar/Cl_2$ plasma.

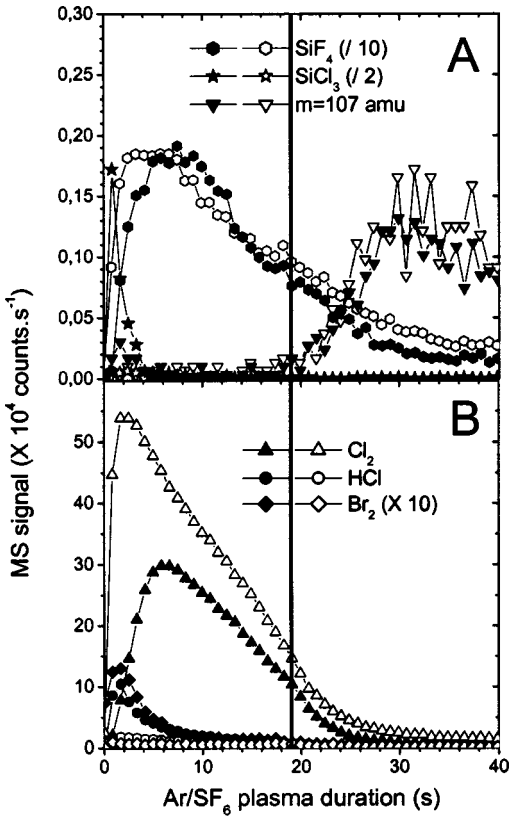


FIG. 12. Time dependent behavior of the gas phase concentration of several species during the layer exposition to the $Ar/SF_6$ plasma (process 3). Full symbol corresponds to the as-deposited $SiO_xCl_y$ layer (same as in Figs. 5–7). Open symbol signals have been obtained under the same condition but after having exposited the layer to an $Ar/Cl_2$ plasma for 1 min (process 4).

Again, these results can be interpreted by assuming that the initial layer is Cl-rich at the surface and more oxidized in the bulk. Consequently, the $Ar/Cl_2$ plasma will etch only the reactive surface layer (forming $SiCl_4$) but the etch reaction will rapidly be stopped when reaching the more oxidized layer's bulk. The subsequent etching of this remaining surface in $Ar/SF_6$ then produces mostly $SiF_4$ etch products and not $SiCl_x$ since without energetic ion bombardment Cl atoms are poorly reactive towards oxidelike surfaces. This explains why the $SiO_xCl_y$ layer is only weakly etched by the $Ar/Cl_2$ plasma, as evidenced in Fig. 12.

The other consequence of exposing the layer to an $Ar/Cl_2$ plasma is a significant modification of its chemical nature at the surface since the deposited layer is nonhomogeneous through its thickness. In particular, the $Ar/Cl_2$ plasma completely eliminates Br atoms from the surface, as evidenced by the strong decrease of $Br_2$ and BrCl (not shown) signals. Similarly, the amplitude of the HCl signal is drastically reduced after the layer exposition to the $Ar/Cl_2$ plasma. This is to be expected since we have previously shown that H and Br atoms are present only near the surface and since this region has been exposed to the $Ar/Cl_2$ plasma. This suggests that while Cl atoms may remove silicon from the Cl-rich reactive surface layer by forming $SiCl_4$, they can also eliminate efficiently H and Br atoms from it. As shown in Fig. 11 this is due to the abstraction reactions forming HCl and BrCl. Finally, Fig. 12(b) shows that the amplitude of the $Cl_2$ signal is almost two times larger after exposing the layer to Cl atoms. This is mostly due to the elimination of H and Br atoms from the layer. In their absence on the surfaces exposed to the plasma, the Cl atoms desorbed from the layer by its fluorination and etching can only recombine with each other resulting in a larger concentration of $Cl_2$ in the gas phase during the first 10 s of the discharge. The difference in the integrated $Cl_2$ signal over the first 10 s allows us to roughly estimate the amount of chlorine that has desorbed from the layer in the form of HCl and BrCl. This amount is approximately 40% of the total number of Cl atoms present in the $SiOCl_x$ layer, as quantified in Sec. III B 2.

## IV. SUMMARY AND CONCLUSION

We have developed a specific plasma diagnostic technique to analyze the chemical composition of the silicon oxychloride layers deposited on the reactor walls during a silicon gate etch process in $HBr/Cl_2/O_2$ chemistry. This layer is essentially a chlorine-rich $SiO_xCl_y$ film, deposited on the walls at a typical rate of 15 $nm \cdot min^{-1}$. However, the layer is not homogeneous through its thickness: it is more Cl, H, and Br rich at the surface, while its bulk is more oxidized. The absence of H and Br from the layer bulk is interesting since the $HBr/Cl_2/O_2$ chemistry contains more than 60% of HBr gas. This density gradient probably results from the abstraction reactions of Cl atoms, forming HCl and BrCl during the layer deposition. As an alternative explanation, Si–Br bonds may be more efficiently oxidized than Si–Cl bonds thus eliminating Br atoms from the layer as it grows. Furthermore we have shown that the $SiO_xCl_y$ layer can be deeply oxidized by exposing it to an $Ar/O_2$ plasma, demonstrating that O atoms can efficiently diffuse through the layer and substitute to Cl atoms deep in the layer. This explains why the $SiO_xCl_y$ layer deposited in the $HBr/Cl_2/O_2$ plasma presents an O density gradient through its thickness. In fact, the bottom of the layer has been exposed to O atoms for a longer time than its surface and then more Si–Cl bonds have been oxidized to form Si–O bonds. Furthermore, this deep layer oxidation mechanism of the film deposited on the entire area of the reactor wall can be considered as an extra source of Cl atoms production for the $HBr/Cl_2/O_2$ plasma. As a result, it is expected that increasing the amount of $O_2$ in the gas mixture will enhance the Cl atom concentration in the gas phase and thus the etch rate. Finally we have shown that the silicon oxychloride layer is poorly affected by an $Ar/Cl_2$ plasma, which can only etch the top Cl, H, and Br rich layer. However, this means that a larger gas phase concentration of Cl atoms should reduce the layer deposition rate by removing the adsorbed $SiCl_x$ species prior to their oxidation.

The technique described above is thus efficient both to analyze the chemical composition of the layers deposited by silicon etching plasmas, and also to analyze their deposition and etching mechanisms. More generally, we underline that it can be used to characterize the walls state of the reactor after a given process. For example, the pure argon sputtering

(or $Ar/SF_6$ chemical sputtering) of the walls after a chamber dry cleaning step (in $SF_6/O_2$) will provide clear information on whether the cleaning has been efficient or not, as no Si or Cl species should be present in a perfectly clean chamber. This analysis can be simply achieved by time resolved actinometry and does not require the use of a mass spectrometer.

## ACKNOWLEDGMENTS

The authors wish to thank O. Joubert and L. Vallier for helpful discussions during the course of these experiments, and for their help in the experimental part of the work.

[1]G. Cunge and J. P. Booth, J. Appl. Phys. **85**, 3952 (1999).
[2]F. H. Bell, O. Joubert, and L. Vallier, J. Vac. Sci. Technol. B **14**, 1796 (1996).
[3]F. H. Bell and O. Joubert, J. Vac. Sci. Technol. B **14**, 2493 (1996).
[4]K. V. Guinn, C. C. Cheng, and V. M. Donnelly, J. Vac. Sci. Technol. B **13**, 214 (1995).
[5]M. Tuda, K. Shintani, and H. Ootera, J. Vac. Sci. Technol. A **19**, 711 (2001).
[6]S. J. Ullal, H. Singh, V. Vahedi, and E. S. Aydil, J. Vac. Sci. Technol. A **20**, 499 (2002).
[7]S. Xu, Z. Sun, X. Qian, J. Holland, and D. Podlesnik, J. Vac. Sci. Technol. B **19**, 166 (2000).
[8]S. Chou, D. Baer, and K. Hanson, J. Vac. Sci. Technol. A **19**, 477 (2000).
[9]S. J. Ullal, A. R. Godfrey, E. A. Edelberg, L. B. Braly, V. Vahedi, and E. S. Aydil, J. Vac. Sci. Technol. A **20**, 43 (2002).
[10]S. Xu, T. Lill, and D. Podlesnik, J. Vac. Sci. Technol. A **19**, 2893 (2001).
[11]C. Lee, D. B. Graves, and M. A. Lieberman, Plasma Chem. Plasma Process. **16**, 99 (1996).
[12]G. Cunge, R. L. Inglebert, O. Joubert, L. Vallier, and N. Sadeghi, J. Vac. Sci. Technol. B **20**, 2137 (2002).
[13]K. Harafuji, M. Ohkuni, M. Kubota, H. Nakagawa, and A. Misaka, IEEE Trans. Electron Devices **46**, 1105 (1999).
[14]J. P. McVittie, S. Abdollahi-Alibeik, and K. C. Saraswat, SPEEDIE 3.0 manual (Stanford University, California, 1996).
[15]A. R. Godfrey, S. J. Ullal, L. B. Braly, E. A. Edelberg, V. Vahedi, and E. S. Aydil, Rev. Sci. Instrum. **72**, 3260 (2001).
[16]S. J. Ullal, H. Singh, J. Daugherty, V. Vahedi, and E. S. Aydil, J. Vac. Sci. Technol. A **20**, 1195 (2002).
[17]W. Schwarzenbach, J. Derouard, and N. Sadeghi, J. Appl. Phys. **90**, 5491 (2001).
[18]R. W. B. Pearse and A. G. Gaydon, *The Identification of Molecular Spectra* (Chapman & Hall, London, 1965).
[19]V. M. Donnelly, J. Vac. Sci. Technol. A **14**, 1076 (1996).
[20]B. Clarenbach, B. Lorenz, M. Krämer, and N. Sadeghi, Plasma Sources Sci. Technol. **12**, 345 (2003).
[21]V. M. Donnelly, J. Appl. Phys. **79**, 9353 (1996).
[22]O. Renault, L. G. Gosset, D. Rouchon, and A. Ermolieff, J. Vac. Sci. Technol. A **20**, 1867 (2002).
[23]M. Schaepkens, N. R. Rueger, J. J. Beulens, X. Li, T. E. F. M. Standaert, P. J. Matsuo, and G. S. Oehrlein, J. Vac. Sci. Technol. A **17**, 3272 (1999).
[24]G. P. Kota, J. W. Coburn, and D. B. Graves, J. Vac. Sci. Technol. A **16**, 270 (1998).
[25]R. Petri, N. Sadeghi, and D. Henry, J. Vac. Sci. Technol. A **13**, 2930 (1995).
[26]K. P. Huber and G. Herzberg, *Constants of Diatomic Molecules* (van Nostrand Reinhold, Toronto, 1979).
[27]V. I. Vedeneyev *et al.*, *Bond Energies, Ionization Potentials, and Electron Affinities* (Edward Arnold, London, 1966).
[28]F. Greer, J. W. Coburn, and D. B. Graves, J. Vac. Sci. Technol. A **18**, 2288 (2000).
[29]L. Vallier, J. Foucher, X. Detter, E. Pargon, O. Joubert, and G. Cunge, J. Vac. Sci. Technol. B **21**, 904 (2003).
[30]S. A. Vitale, H. Chae, and H. H. Sawin, J. Vac. Sci. Technol. A **19**, 2197 (2001).
[31]L. Desvoivres, O. Joubert, and L. Vallier, J. Vac. Sci. Technol. B **19**, 420 (2001).
[32]K. Nojiri, K. Tsunokumi, and K. Yamazaki, J. Vac. Sci. Technol. B **14**, 1791 (1996).
[33]N. Ozawa, T. Matsui, and J. Kanamori, Jpn. J. Appl. Phys., Part 1 **34**, 6815 (1995).